2016 IEEE 55th Conference on Decision and Control (CDC)
ARIA Resort & Casino
December 12-14, 2016, Las Vegas, USA

Online Optimal Gait Generation for Bipedal Walking Robots using Legendre Pseudospectral Optimization

Ayonga Hereid[1], Shishir Kolathaya[1] and Aaron D. Ames[2]

***Abstract*— This paper presents an optimal gait synthesis method that exploits the full body dynamics of robots using the Hybrid Zero Dynamics (HZD) control framework and—for the first time—experimentally realizes online HZD gait generation for a planar underactuated robot. Hybrid zero dynamics is an established theoretical framework that formally enables stable control of dynamic locomotion by enforcing virtual constraints through feedback controllers. An essential part of successfully realizing dynamic walking with HZD framework is determining parameters of the virtual constraints that satisfy hybrid invariant condition via nonlinear constrained optimization. Due to the complexity of the full hybrid system model of the robot, these optimization problems often suffer from slow convergence and local minima. In this paper, we improve the reliability of the HZD gait optimization and significantly increase the convergence speed by taking advantage of the direct transcription formulation and the exponential convergence of the global orthogonal collocation (a.k.a. pseudospectral) method. As a result, generating HZD gaits online becomes feasible with an average computation time less than 0.5 seconds, as will be demonstrated experimentally on a bipedal robot.**

I. Introduction

The goal of bipedal robots is to demonstrate dynamic and agile locomotion that allows for navigation of terrain not approachable by wheeled robots. Yet the ability to accommodate changes in terrain present in uncontrolled environments, however, is a challenging problem. The difficulty arises from the fact that planning dynamic motions that are consistent with the full body dynamics of the complex robot model is often computationally expensive. This paper presents a novel optimization formulation which enables existing nonlinear programming (NLP) solvers to generate dynamic gaits online within the HZD framework, and experimentally evaluated this method on an underactuated planar robot, DURUS-2D.

Existing methods of motion planning typically use reduced-order models—such as the linear inverted pendulum model (LIPM)—to mitigate the complexity of full body dynamics. By balancing the robot about the Zero Moment Point (ZMP), these approaches plan trajectories for the simplified model and then generate the whole body motion by conforming the robot to these analytically tractable dynamics [12], [15]. These simplifications, however, place stringent requirements on the design of the robot (e.g. all joints must be actuated with no significant compliance) and restrictions on the overall locomotion capabilities of the machine (e.g. the robot must always walk with a constant COM height). Embracing planning and formal control that exploits the full body dynamics of the robot is a path toward unlocking the fully dynamic capabilities of the machine. An increasing number of methods have been developed to generate optimal gaits using full body dynamics optimization [13], [16]. Some researchers also explore a middle path, in which whole body motion is planned with the robot's centroidal dynamics subject to full body kinematic constraints [5]. While the whole-body optimization methods can realize more dynamic behaviors, the process requires excessive amount of time and may not be able to converge reliably, and therefore, are only suitable for off-line *a priori* motion planning.

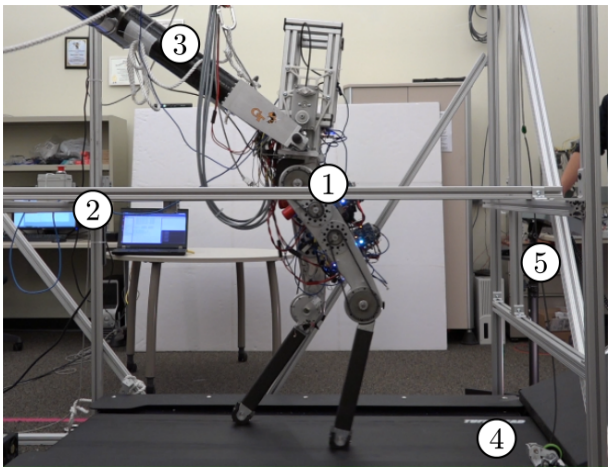

Fig. 1: Experimental setup of the DURUS-2D walking on a treadmill. The labels represents: (1) DURUS-2D robot, (2) the control workstation, (3) the linear boom used to constrain DURUS-2D to the saggital plane, (4) the treadmill whose velocity is measured by an encoder attached, (5) the control panel used to change the velocity of the treadmill.

Hybrid zero dynamics (HZD) [21] is a formal framework that utilizes the full-order dynamics of the hybrid system model by synthesizing feedback controllers that yield periodic dynamic locomotion even in the presence of underactuation [4], [10], [19] and multi-contact foot behaviors [22]. In the HZD framework, a set of *virtual constraints* enforced via nonlinear feedback controllers, formally yielding a low-dimensional representation of the system which captures the stability properties of full order dynamics if the virtual constraints are invariant through impact. Hence the planning of

This research is supported by DARPA grant D15AP00006 and NSF grants CPS-1239055 and NRI-1526519.

[1]Ayonga Hereid and Shishir Kolathaya are with the Woodruff School of Mechanical Engineering, Georgia Institute of Technology, Atlanta, GA, 30332 USA

[2]Aaron D. Ames is with the Woodruff School of Mechanical Engineering and the School of Electrical and Computer Engineering, Georgia Institute of Technology, Atlanta, GA, 30332 USA

HZD gaits can be transformed into a nonlinear optimization that determines the parameters of virtual constraints satisfying a hybrid invariance condition. However, existing methods for generating such gaits are often time consuming, and thus must be performed off line. While advanced control methods [3], [9], [14] have been developed to robustify the gait under perturbations and switch between gaits (often encoded as *motion primitives*) [17], these methods are restricted to a limited number of gaits generated in advance.

In this paper, we present an online HZD gait generation method using the *pseudospectral* optimization formulation. Exploiting the advantages of direct transcription formulation of the pseudospectral method, we formulate the HZD gait optimization in a fashion that makes it amendable to being solved in a fast and reliable fashion utilizing existing NLP solvers. More importantly, the proposed approach opens the possibility of generating optimal gaits online while considering the whole body dynamics of the robot. We experimentally evaluate the performance of this method on a planar underactuated robot which walks on a treadmill with varying speeds. As a result, the optimizer successfully generates gaits with different walking speeds online to enable the robot to adjust to the changing speed of the treadmill—this provides the first example of online HZD gait generation.

II. Hybrid Zero Dynamics Framework

This section will focus on the *hybrid zero dynamics* (HZD) control framework that will be utilized to achieve stable periodic orbits in systems with impact. The formal definitions in this section provide the necessary structure for formulating the fast HZD gait optimization problem.

A. Bipedal Walking as a Hybrid System

Dynamic bipedal locomotion is often modeled as a hybrid control system in literature, wherein walking consists of an alternating sequence of continuous and discrete events [2]. Here, we consider the robot of interest, the 5-link underactuated planar robot, DURUS-2D. Let $\mathcal{Q}$ be the configuration space of the robot with coordinates $q \in \mathcal{Q}$ (see Fig. 2a), the *hybrid control system* is given as a tuple [2],

$$\mathscr{HC} = (\mathcal{D}, \mathcal{U}, S, \Delta, FG), \tag{1}$$

where $\mathcal{D} \subseteq T\mathcal{Q} \times \mathcal{U}$ is an admissible domain, $\mathcal{U} \subseteq \mathbb{R}^4$ is a set of admissible controls, $S \subset \mathcal{D}$ is a *guard* that determines the switching surface of discrete events, $\Delta : \pi(S) \to \pi(\mathcal{D} \backslash S)$ is a smooth *reset map* with $\pi : \mathcal{D} \to T\mathcal{Q}$ a canonical projection, and FG is the affine control system defined on $\mathcal{D}$, i.e., $\dot{x} = f(x) + g(x)u$ with $(x, u) \in \mathcal{D}$ and $u \in \mathcal{U}$, where $x = (q, \dot{q})$ is the set of states. A graphic demonstration of the single-domain hybrid system model is shown in Fig. 2b.

Continuous Dynamics. With the mass, inertia and length properties of each link of the planar DURUS-2D model, the constrained continuous dynamics of the system can be determined by the classical Euler-Lagrange equation [8]:

$$D(q)\ddot{q} + H(q, \dot{q}) = Bu + J^T(q)F, \tag{2}$$

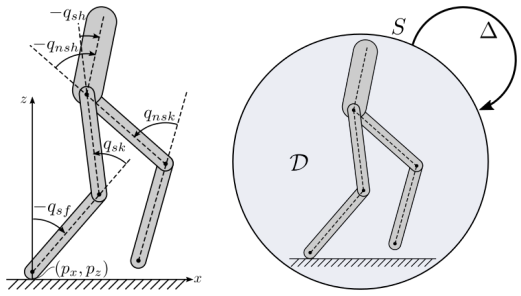

(a) Robot Coordinates (b) Hybrid System Model

Fig. 2: Model configuration of the DURUS-2D robot.

where $D(q)$ is the inertia matrix, $H(q, \dot{q}) = C(q, \dot{q})\dot{q} + G(q)$ is the vector containing the Coriolis, centrifugal and the gravity terms, B is the actuator distribution matrix, and $F : T\mathcal{Q} \times U \to \mathbb{R}^2$ is a vector of ground reaction forces that satisfy the contact conditions: $\eta(q) = (p_x, p_z) \equiv 0$. To maintain the ground contact, the reaction forces F should satisfy the holonomic constraints, i.e.,

$$J(q)\ddot{q} + \dot{J}(q, \dot{q})\dot{q} = 0, \tag{3}$$

with $J(q) = \frac{\partial \eta(q)}{\partial q}$.

Domain of Admissibility. The admissible conditions of the domain $\mathcal{D}$ is determined by unilateral constraints of the system. For example, the foot contact is considered to be a unilateral constraint. The reaction forces must satisfy the friction cone constraints and the normal force should be positive. In addition, the non-stance foot must be above the ground throughout a step. We formulate these conditions in terms of inequalities, given as

$$A(q, \dot{q}, u) = \begin{bmatrix} \mathcal{R}F(q, \dot{q}, u) \\ h_{nsf}(q) \end{bmatrix} \geq 0, \tag{4}$$

where $\mathcal{R}$ is a constant matrix capturing the friction cone and the positive normal force constraints. Hence, the domain of admissibility is defined as:

$$\mathcal{D} = \{(q, \dot{q}, u) \in T\mathcal{Q} \times U | A(q, \dot{q}, u) \geq 0\}. \tag{5}$$

The guard $S \subset \mathcal{D}$ at which the discrete event occurs is a co-dimensional one submanifold of the domain. Let $h : \mathcal{D} \to \mathbb{R}$ be an appropriate element of (4) associated with the discrete event, the guard is defined as

$$S = \{(q, \dot{q}, u) \in \mathcal{D} | h_{nsf}(q)(q, \dot{q}, u) = 0, \dot{h}_{nsf}(q, \dot{q}, u) < 0\}.$$

Discrete Dynamics. A discrete event occurs when the non-stance foot hits the ground. We assume the impact is perfectly plastic [11]. Configurations of the system are invariant through the impact, i.e., $q^+ = \mathscr{R}q^-$ with $\mathscr{R}$ be the relabeling matrix that swaps the left and the right leg at every step [2]. Post-impact velocities must satisfy the plastic impact equation:

$$\begin{bmatrix} D(q) & -J^T(q) \\ J(q) & 0 \end{bmatrix} \begin{bmatrix} \dot{q}^+ \\ \delta F \end{bmatrix} = \begin{bmatrix} D(q)\dot{q}^- \\ 0 \end{bmatrix}, \tag{6}$$

where δF are impulsive forces. Solving (6) yields the reset map $(q^+, \dot{q}^+) = \Delta(q^-, \dot{q}^-)$.

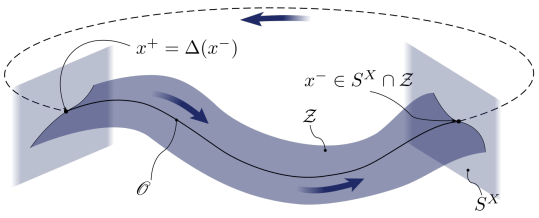

Fig. 3: A periodic orbit on the Hybrid Zero Dynamics.

B. Hybrid Zero Dynamics

In the hybrid zero dynamics framework, virtual constraints are introduced as a means to synthesize feedback controllers that realize stable and robust locomotion in underactuated robots. By designing virtual constraints that are invariant through impact, an invariant submanifold is created—termed the *hybrid zero dynamics surface*—wherein the evolution of the system is dictated by the low-dimensional hybrid dynamical system [2], [21]. The focus of this subsection is to derive conditions under which hybrid zero dynamics can be realized in the bipedal robot.

Virtual Constraints. *Virtual constraints* are defined as the difference between the actual and the desired outputs of the robot:

$$y_2 = y_2^a(q) - y_2^d(\theta(q), \alpha), \tag{7}$$

where y_2 is (vector) relative degree 2 by definition. In this paper, we pick actuated joint angles as our actual outputs,

$$y_2^a(q) = (q_{sk}, q_{sh}, q_{nsh}, q_{nsk}). \tag{8}$$

Desired outputs, y_2^d, are defined in terms of 5-th order Bézier polynomials parameterized by α and θ is a strictly monotonic state-based parameterization of time.

Feedback Controller. With the goal of driving the virtual constraints $y_2 \to 0$ exponentially, we consider the feedback linearzation controller [2]:

$$u^{(\alpha,\varepsilon)} = -(L_g L_f y_2)^{-1}(L_f^2 y_2 + 2\varepsilon L_f y_2 + \varepsilon^2 y_2) \tag{9}$$

with a control gain $\varepsilon > 1$, where L_f and L_g are Lie derivatives. Applying this control law to the hybrid control system in (1) results in linear output dynamics:

$$\ddot{y}_2 = -2\varepsilon L_f y_2 - \varepsilon^2 y_2. \tag{10}$$

This yields a *hybrid system* of (1) with $\mathcal{U} = \emptyset$, given as,

$$\mathscr{H}^{(\alpha,\varepsilon)} = (\mathcal{D}^X, S^X, \Delta, F^{(\alpha,\varepsilon)}), \tag{11}$$

where $\mathcal{D}^X \subset T\mathcal{Q}$ is an admissible domain, S^X is a *guard* with $S^X \subset \mathcal{D}^X$, and $F^{(\alpha,\varepsilon)}$ is a dynamical system defined on $\mathcal{D}^X$, i.e., $\dot{x} = f^{(\alpha,\varepsilon)}(x) = f(x) + g(x)u^{(\alpha,\varepsilon)}$ with $x \in \mathcal{D}^X$.

Periodic Orbit. For the hybrid system $\mathscr{H}^{(\alpha,\varepsilon)}$, let $\varphi_t(x)$ be a flow of the continuous dynamics $F^{(\alpha,\varepsilon)}$ in (11). For $x^* \in S$, we say that $\varphi_t(x)$ is hybrid periodic if there exists a finite $T > 0$ such that $\varphi_T(\Delta(x^*)) = x^*$. A set $\mathscr{O} \subset \mathcal{D}^X$ is a hybrid periodic orbit if $\mathscr{O} = \{\varphi_t(\Delta(x^*)) : 0 < t < T\}$ for a hybrid periodic flow $\varphi_t(x)$ (see Fig. 3). Further, x^* is the fixed point, if the periodic orbit $\mathscr{O}$ is *transversal* to S^X in exactly one point x^*. For the stability of periodic orbits in the context of Lyapunov, we refer the readers to [3].

Hybrid Zero Dynamics. With the feedback control law in (9), the *zero dynamics* submanifold,

$$\mathcal{Z} = \{(q, \dot{q}) \in \mathcal{D}^X | y_2 = 0, \dot{y}_2 = 0\}. \tag{12}$$

is rendered invariant in the continuous domain. However, it is not necessarily invariant through discrete dynamics without carefully designing the virtual constraints. Therefore, if there exist a set of parameters α so that the submanifold $\mathcal{Z}$ is impact invariant, i.e.,

$$\Delta(x) \in \mathcal{Z}, \qquad \forall x \in S^X \cap \mathcal{Z}, \tag{13}$$

then we call $\mathcal{Z}$ the *hybrid zero dynamics* surface. That is, any solution that starts in $\mathcal{Z}$ remains in $\mathcal{Z}$, inspite of the impacts in $\mathcal{Z}$, see Fig. 3. As a result, the behavior on this reduced dimensional space can be used to encode the full-order behavior of the bipedal humanoid robot. Therefore, the goal is to find a set of parameters α that satisfies the HZD constraints in (13). Importantly, the end result is a means of formally encoding and realizing dynamic walking gaits.

III. Online HZD Gait Optimization

In this paper, we employ the global orthogonal collocation—often termed as *pseudospectral methods*—to formulate a computationally fast and reliable HZD gait optimization problem for an underactuated biped. The pseudospectral methods first approximate then solve algebraic collocation equalities at particularly collocated discrete nodes to obtain the flow of the dynamical systems [6]. This feature significantly reduces the computational expense of the time-marching forward integration of system dynamics, and hence, increases the convergence speed remarkably as compared to existing direct shooting optimization methods [2]. In addition, this formulation enables the use of defect variables by which the constraint expressions can be further simplified, so that the analytic Jacobian, even Hessian, of the optimization problem can be determined. These methods will form the basis for the experimental realization of online gait generation.

A. Legendre Pseudospectral Method

The fundamental idea behind the Legendre pseudospectral method is to approximate the solution of the dynamical system, $\dot{x} = f(x)$, by N^{th} order Lagrange interpolating polynomials which interpolate the solutions at Legendre-Gauss-Lobatto (LGL) nodes. The LGL nodes are defined as zeros of $(\tau^2 - 1)\dot{L}_N(\tau)$ distributed on the interval $\tau \in [-1, 1]$, where $\dot{L}_N(\tau)$ is the derivative of the N^{th} order Legendre polynomial $L_N(\tau)$ [7]. Let $x_i = (q_i, \dot{q}_i)$ be approximated states at node τ_i with $i \in [0, N]$, then the solution $x(\tau)$ on $\tau \in [-1, 1]$ is approximated by

$$x(\tau) \approx \bar{x}(\tau) = \sum_{i=0}^{N} x_i \phi_i(\tau) \tag{14}$$

where $\phi_i(\tau) = \frac{1}{N(N+1)L_N(\tau_i)} \frac{(\tau^2-1)\dot{L}_N(\tau)}{\tau-\tau_i}$ is the Lagrange interpolating polynomial of order N. It can be noted that $\phi_i(\tau_k) = 1$, if $i = k$ and $\phi_i(\tau_k) = 0$ if $i \neq k$. Similarly, the derivative of $x(\tau)$ is approximated by differentiating the approximation $\bar{x}(\tau)$ in (14). Interestingly, the derivative of $\phi_i(\tau_k)$ at any LGL node τ_k is a constant determined only by i and k [18]. This feature leads to the LGL differentiation matrix $\mathbf{D}^{\mathrm{LGL}} \in \mathbb{R}^{(N+1)\times(N+1)}$. Let $\mathbf{D}^{\mathrm{LGL}}_{ki} = \dot{\phi}_i(\tau_k)$ be the (k,i) entry of the differentiation matrix, we have

$$\mathbf{D}^{\mathrm{LGL}}_{ki} = \begin{cases} \frac{L_N(\tau_i)}{L_N(\tau_k)(\tau_i-\tau_k)}, & \text{if} \quad i \neq k, \\ -\frac{N(N+1)}{4}, & \text{if} \quad i = k = 0, \\ \frac{N(N+1)}{4}, & \text{if} \quad i = k = N, \\ 0, & \text{otherwise.} \end{cases} \tag{15}$$

The collocation condition is defined such that at all LGL nodes the approximated derivatives, $\dot{\bar{x}}(\tau_k)$, equal to the derivatives that are computed from the system dynamics, $f(x(\tau_k))$. In other words, the NLP solver is set to find a set of discrete states $\mathbf{X} = [x_0^T \ x_1^T \cdots x_N^T]^T$ that satisfy the constraints given by

$$(\mathbf{D}^{\mathrm{LGL}} \otimes \mathbf{I})\mathbf{X} - \mathbf{F}[\mathbf{X}] = 0, \tag{16}$$

where $\otimes$ represents the Kronecker products, $\mathbf{I}$ is an identity matrix, and $\mathbf{F}[\mathbf{X}] = [f(x_0)^T \ f(x_1)^T \cdots f(x_N)^T]^T$. Different from the standard collocation schemes, the pseudospectral method provides an approximation of the solution that has exponential convergence (as a rate of the number of LGL nodes) to the smooth solution [18].

More importantly, by expressing the forward integration with closed-form equality constraints, the pseudospectral method enables the introduction of defect variables to expedite the problem evaluation even faster. Defect variables are supplementary decision variables that could be computed in closed-form initially. For instance, instead of computing $\dot{x}$ in (16) from the dynamical equations we introduce the derivatives as augmented NLP decision variables and then enforce the dynamical equations as equality constraints of x and $\dot{x}$. It would decouple the complex constraints into multiple simpler constraints, as a result, significantly simplifies the constraint expression such that determining the analytical Jacobian of constraints becomes feasible [10]. In nonlinear programming problems, providing analytical Jacobian of constraints would significantly increase the computation speed and improve the robustness of the optimization convergence.

B. Fast HZD Gait Optimization

The goal of the HZD gait optimization is to find an optimal periodic orbit on the hybrid zero dynamics surface that is determined by virtual constraints parameters α. Here, we construct the problem based on the pseudospectral method described in the previous section.

Let $0 = t_0 < t_1 < \cdots < t_N = T$ be the time points correspond to N^{th} order LGL nodes, where T is the period of the periodic orbit. Let q_k, $\dot{q}_k$, $\ddot{q}_k$, u_k, and F_k are the discrete joint angles, velocities, and acceleration, control inputs and ground reaction forces needed to be determined by the NLP solver at each node t_k. With the introduction of these defect variables, the collocation constraints in (16) becomes:

$$(\mathbf{D}^{\mathrm{LGL}} \otimes \mathbf{I})\mathbf{X} - \frac{T}{2}\dot{\mathbf{X}} = 0, \tag{C1}$$

where the $\frac{T}{2}$ is due to the affine transformation of the time [7]: $t = \frac{T}{2}(\tau + 1)$. To guarantee that $\dot{x}_k$ indeed satisfies the closed-loop dynamics, here we use the approach described in [10]. Specifically, the constrained Lagrangian dynamics equation in (2), holonomic constraints in (3), and output dynamics in (10) are imposed to equivalently (and fully) represent the closed loop dynamics $f^{(\alpha,\varepsilon)}(x)$. Thus, we have following equalities:

$$D(q_k)\ddot{q}_k + H(q_k, \dot{q}_k) - Bu_k - J^T(q_k)F_k = 0, \tag{C2}$$

$$J(q_k)\ddot{q}_k + \dot{J}(q_k, \dot{q}_k)\dot{q}_k = 0, \tag{C3}$$

$$\ddot{y}_2(q_k, \dot{q}_k, \ddot{q}_k, \alpha) + 2\varepsilon\dot{y}_2(q_k, \dot{q}_k, \alpha) + \varepsilon^2 y_2(q_k, \alpha) = 0, \tag{C4}$$

for all $k \in \{0, 1, \ldots, N\}$. It can be noted that the holonomic constraints in (C3) determines the constraint wrenches when coupled with (C2), and (C4) determines u_k implicitly without the explicit calculation of the feedback control law given in (9). The result is a set of smooth control inputs that drives $y_2 \to 0$ given $\varepsilon > 0$.

In addition, the solution should always lies on the specified admissible domain manifold and $x_N \in S$. Hence, we enforce

$$A(x_k, u_k, F_k) \geq 0, \quad \forall k \in \{0, 1, \ldots, N\}, \tag{C5}$$

$$h(x_N) = 0, \quad \dot{h}(x_N) < 0 \tag{C6}$$

Note that the constraints (C5) now can be stated directly in terms of F_k, resulted in much simpler expressions.

To make sure the solution is periodic, we enforce equality constraints between states at the first and last node that satisfy the rigid impact equation given in (6), i.e.,

$$q_0 - \mathscr{R}q_N = 0, \tag{C7}$$

$$J(q_0)\mathscr{R}\dot{q}_0 = 0, \tag{C8}$$

$$D(q_0)(\dot{q}_0 - \mathscr{R}\dot{q}_N) - J^T(q_0)\delta F = 0. \tag{C9}$$

Moreover, the hybrid invariance constraints can be directly imposed on the states at the first node.

$$y_2(q_0, \alpha_0) = 0, \tag{C10}$$

$$\dot{y}_2(q_0, \dot{q}_0, \alpha_0) = 0. \tag{C11}$$

Finally, the contact constraints must equal the desired constants (for DURUS-2D walking, the constants are zero):

$$\eta(q_0) = 0 \tag{C12}$$

The constraints defined in (C1)–(C12) place the necessary requirements for the HZD gait optimization. With simpler constraints thanks to the defect variables, we are able to rigorously compute analytic expressions of the gradient of the cost function and the Jacobian of the constraints, even the Hessian of the optimization problem, using any proper symbolic mathematics software. The end result is a fast and reliably converging nonlinear programming problem for generating dynamic walking gaits for the DURUS-2D robot within the hybrid zero dynamics framework.

IV. Speed Regulation via Online Optimal Gait Generation

In this section, we employ the gait generation formulation to design optimal gaits online. In particular, we optimize new HZD gaits subject to a specific desired forward velocity that changes when the robot is still walking, and apply the newly optimized gait parameters α^* to change the walking velocity of the robot in real time.

Objective Oriented Constraints. We start with formulating objective oriented (OC) constraints for this particular purpose. For periodic walking gaits, the distance travelled during a step equals the step length of the gait. Let $\bar{v}^d$ be the desired forward speed of the robot, the optimized gait should satisfy the following condition:

$$\|\frac{L_{step}(q_N)}{T} - \bar{v}^d\| \leq \delta \tag{OC1}$$

for a small constant $\delta > 0$, where $L_{step}(q_N) = p^x_{nsf}(q_N)$ is the step length and $p^x_{nsf}(q)$ is the x-position of the non-stance foot. With a goal to apply optimized gaits to the robot hardware on the fly, additional constraints must be enforced so that the resulting gaits are reasonable and feasible from the viewpoint of the actual hardware. In particular, we consider the following constraints.

- The torso should move within a reasonable range, i.e., given $q_{tor}(q) = -q_{sf} - q_{sk} - q_{sh}$,

$$q^{\min}_{tor} \leq q_{tor}(q) \leq q^{\max}_{tor}. \tag{OC2}$$

- There should be enough swing foot clearance to prevent scuffing, Hence we constrain that the non-stance foot is always above a predetermined curve:

$$h_{nsf}(q) - h^d_{nsf}(q) \geq 0, \tag{OC3}$$

  where $h^d_{nsf}(q)$ is the desired foot clearance curve.
- The joint velocities and actuator torques must be within the specifications of the motors:

$$-\dot{q}^{\max} \leq \dot{q} \leq \dot{q}^{\max}, \tag{OC4}$$
$$-u^{\max} \leq u \leq u^{\max}. \tag{OC5}$$

Energy Efficient Gait Optimization. With a goal of achieving energy efficient locomotion at a specific speed, the cost function of the NLP is defined as the mechanical cost of transport of the gait, given as:

$$\Phi := \frac{1}{mgL_{step}(q_N)} \sum_{k=0}^{N} w_k P(u_k, \dot{q}_k) \tag{17}$$

where w_k are the LGL weights given by

$$w_k = \frac{2}{N(N+1)} \frac{1}{L_N(\tau_k)]^2}, \tag{18}$$

and $P(u, \dot{q})$ is the total power of the actuated joints:

$$P(u, \dot{q}) = \|u \circ (B^T \dot{q})\|^2. \tag{19}$$

Let $\mathbf{Z} = \{\alpha, T, \mathscr{Z}, \delta F\}$ be the set of augmented decision variables, where $\mathscr{Z} = \{(q_k, \dot{q}_k, \ddot{q}_k, u_k, F_k) : 0 \leq k \leq N\}$, and $\mathbf{C}(\mathbf{Z})$ as a vector of constraints given in (C1)–(C12) and (OC1)–(OC5), we state the speed regulated HZD gait optimization problem as,

$$\begin{aligned} \mathbf{Z}^* = \ & \underset{\mathbf{Z}}{\operatorname{argmin}} \ \Phi(\mathbf{Z}) \\ \text{s.t} \quad & \mathbf{C}^{\min} \leq \mathbf{C}(\mathbf{Z}) \leq \mathbf{C}^{\max} \\ & \mathbf{Z}^{\min} \leq \mathbf{Z} \leq \mathbf{Z}^{\max} \end{aligned} \tag{20}$$

This HZD gait generation NLP is then solved using IPOPT with linear solver `ma57` [20].

V. Experimental Results

In this section, we present the experimental results of the online speed regulation optimization that we have proposed in the previous section.

Experimental Setup. As shown by Fig. 1, the boom is mounted on the cage along with the robot. The boom constraints the robot motion to the lateral plane (front-back and up-down motions only). The boom structure is freely allowed to slide on the cage in order to ensure that the robot motion is not restricted in its general direction of walking. The off board processing unit is connected to the joint drives via ETHERCAT. The desired joint angles and velocities are generated by the off board processing unit in real time using the optimal gait parameters α^* from the gait optimization, and sent to the local controller at the rate of 1 kHz. The treadmill speed is changed from its control panel, while the actual speed is measured by an encoder and the readings are updated and sent to the off board unit at the same rate.

To begin with, we use the exact same optimization formulation to generate a nominal gait offline. The desired walking speed of the nominal gait is chosen to be $0.65\ m/s$. The offline optimization that seeded with random initial guesses converges to an optimal solution successfully with an average CPU time of 9.5 seconds. The optimization results presented in this paper are obtained by running IPOPT on a laptop computer with an Intel Core i7-3820QM processor (2.7 GHz) and 12 GB of RAM. In particular, no parallel computation is enabled in all tests.

Performance of Online Optimization. The measured treadmill speed serves as the desired speed $\bar{v}^d$ in (20) and is published to a ROS message at the beginning of every step. Once the online gait optimizer, which runs on the same laptop computer, receives a new message from the ROS message, the optimizer runs a new optimization subject to the new desired walking speed if the difference between the updated speed and previously optimized speed is greater than a certain threshold. In particular, we pick both the threshold and the δ in (OC1) to be 0.01. Once the optimization converges, new gait parameters are sent to the off board processing unit immediately and applied to the gait controller at the beginning of the next robotic step. For the experimental results reported in this paper, we started from the nominal gait and then changed the treadmill speed from its control panel within a range from $0.43\ m/s$ to $0.97\ m/s$. The treadmill speed was slowed down and speeded up multiple

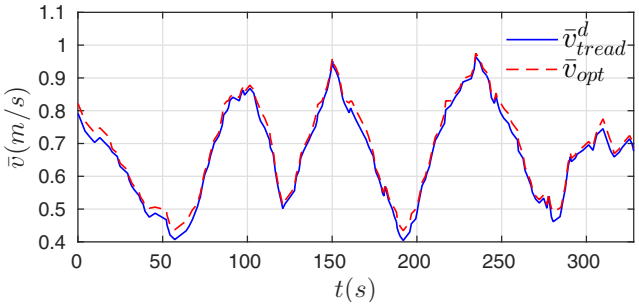

Fig. 4: Tracking of varying treadmill speed, $\bar{v}_{tread}^{d}$. The dashed line represents the speed, $\bar{v}_{opt}$, of the optimazed gait.

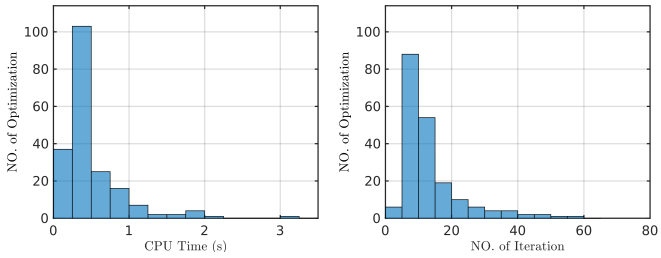

(a) Runtime (b) Iteration

Fig. 5: The histogram plots of total 198 gait optimizations.

times, as the blue line shown in Fig. 4. The dashed red line in Fig. 4 showed that the online optimizer generates new gaits that closely tracked the desired walking speed.

In order to achieve faster convergence, we enabled the `warm start` feature of the optimizer in IPOPT where we used the result from the previous optimization as the initial guess of the next optimization. Further we provided the exact Hessian of the problem using the analytical second order derivatives of constraints and cost function instead of the Quasi-Newton approximation of the Hessian. By doing so, the optimizations converged faster and more reliably. Fig. 6 shows the histogram figures of the CPU time spent and total number of iterations of each optimization. The average CPU time spent of the total 198 gait optimizations during the experiment of 328 seconds is 0.4964 second, which is less than the average time of one step. There are only two occasions when the optimizer ran more than 2 seconds. Furthermore, the online optimizer converged successfully to an optimal solution in all occurrences within the maximum allowed iterations of 100. In fact, the average number of iterations is just 13 with the maximum being 67. The video demonstration of the experiment can be found in [1].

The performances of the online gait optimization when providing the exact and Quasi-Newton approximation of the Hessian are also studied. The comparison results are shown in Table I, in which the optimizer spent more time and required more iterations to converge. Further, in 50 of total 198 occurrences when using the Quasi-Newton approximation, the optimization stalled at an almost feasible solution, which is indicated as the "`Restoration Failed`" in IPOPT

TABLE I: Performance comparison of online gait optimization with different approaches to computing the Hessian.

Method	CPU Time (sec)		NO. of Iteration	
	Average	Std.	Average	Std.
Exact Hessian	0.4954	0.3997	13.1414	10.13
Quasi-Newton	0.8927	0.8749	44.5657	36.60

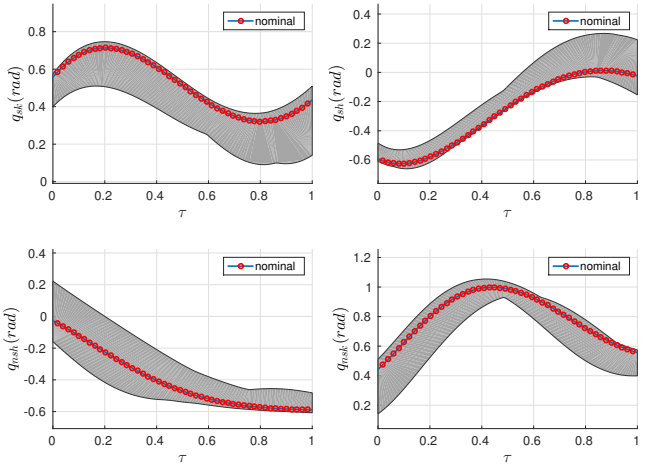

Fig. 6: The gray areas represent desired outputs of optimal gaits at different walking speeds generated by the online optimizer. The blue lines with red circles show the desired outputs of the nominal gait.

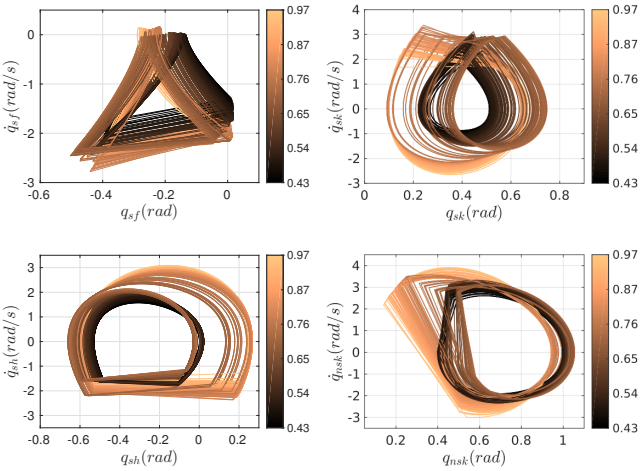

Fig. 7: Phase portraits of optimal gaits at different walking speeds generated by the online optimizer. The color bar indicates the speed of the gaits, where darker lines represent slower speeds and lighter lines represent faster speeds.

outputs [20]. These failures do not occur when we were using the exact Hessian for the problem.

Gait Performance. With the proper objective-orientated constraints presented in Sec. IV, all gaits generated from the online optimizer are physically realizable on the DURUS-2D hardware. Fig. 8 shows the snapshots of the gaits during the speed regulated walking experiment. Fig. 6 shows the range of desired outputs of all gaits generated. These gray areas

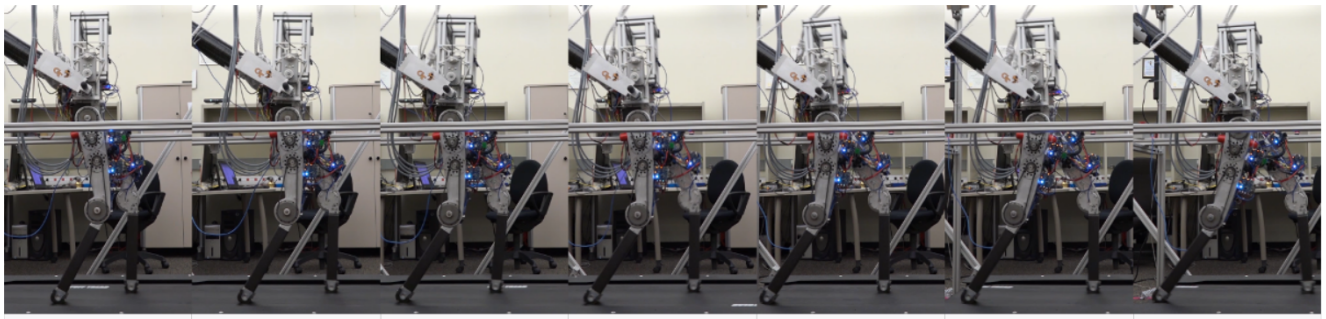

Fig. 8: Snapshots of optimal gaits generated from the online optimizer at different walking speeds.

are then compared to the desired outputs of the nominal gait, which shows very good similarities. Fig. 7 shows the phase portraits of robot joints for all gaits generated, where darker lines represent the slower gaits and lighter lines represent the faster gaits. It can be noted that each gait produces periodic orbits for the robot joints. Also, the size of the orbits is expanded when the speed of the robot is increased, which shows that the optimizer generated gaits with faster joint velocities and wider joints movements as the speed increased.

VI. Conclusion

This paper presented an online gait optimization approach for generating dynamic locomotion on an underactuated robot under the hybrid zero dynamics framework. Building upon the theoretical foundation of HZD, this method optimizes the interactions of the full body dynamics of the hybrid system model. More importantly, the utilization of the state-of-the-art pseudospectral method empowers a fast and reliable gait optimization method which is, for the first time, capable of generating HZD gaits online. We experimentally validated the optimization method on a planar 5-link underactuated robot subjecting to varying desired walking speeds. The online full body dynamics optimizer successfully optimized energy-efficient walking gaits in an average of 0.5 seconds, while satisfying all dynamical and kinematics constraints.

References

[1] Online optimal gait generation for bipedal walking robots using Legendre pseudospectral optimization: https://youtu.be/pvH3c2G2Pj4.

[2] A. D. Ames. Human-inspired control of bipedal walking robots. *IEEE Transactions on Automatic Control*, 59(5):1115–1130, May 2014.

[3] A. D. Ames, K. Galloway, K. Sreenath, and J. W. Grizzle. Rapidly exponentially stabilizing control Lyapunov functions and hybrid zero dynamics. *IEEE Transactions on Automatic Control (TAC)*, 59(4):876–891, April 2014.

[4] B. G. Buss, A. Ramezani, K. Akbari Hamed, K. S. Griffin, B. A., Galloway, and J. W. Grizzle. Preliminary Walking Experiments with Underactuated 3D Bipedal Robot MARLO. In *Intelligent Robots and Systems (IROS 2014)*, pages 2529–2536. IEEE, 2014.

[5] Hongkai Dai, Andrés Valenzuela, and Russ Tedrake. Whole-body motion planning with centroidal dynamics and full kinematics. In *2014 14th IEEE-RAS International Conference on Humanoid Robots (Humanoids)*, pages 295–302. IEEE, 2014.

[6] Gamal Elnagar, Mohammad Kazemi, and Mohsen Razzaghi. The pseudospectral Legendre method for discretizing optimal control problems. *Automatic Control, IEEE Transactions on*, 40(10):1793–1796, 1995.

[7] Qi Gong, Wei Kang, and M. I. Ross. A pseudospectral method for the optimal control of constrained feedback linearizable systems. *Automatic Control, IEEE Transactions on*, 51(7):1115–1129, 2006.

[8] J. W. Grizzle, C. Chevallereau, R. W. Sinnet, and A. D. Ames. Models, feedback control, and open problems of 3D bipedal robotic walking. *Automatica*, 50(8):1955 – 1988, 2014.

[9] K. A. Hamed and J. W. Grizzle. Robust event-based stabilization of periodic orbits for hybrid systems: Application to an underactuated 3D bipedal robot. In *American Control Conference (ACC), 2013*, pages 6206–6212, June 2013.

[10] A. Hereid, E. A. Cousineau, C. M. Hubicki, and A. D. Ames. 3D dynamic walking with underactuated humanoid robots: A direct collocation framework for optimizing hybrid zero dynamics. In *2016 IEEE International Conference on Robotics and Automation (ICRA)*, pages 1447–1454, May 2016.

[11] Y. Hurmuzlu and D. B. Marghitu. Rigid body collisions of planar kinematic chains with multiple contact points. *The International Journal of Robotics Research*, 13(1):82–92, 1994.

[12] S. Kajita *et al.* Biped walking pattern generation by using preview control of zero-moment point. In *IEEE International Conference on Robotics and Automation*, volume 2, pages 1620–1626. IEEE, 2003.

[13] Igor Mordatch, Kendall Lowrey, and Emanuel Todorov. Ensemble-CIO: full-body dynamic motion planning that transfers to physical humanoids. In *2015 IEEE/RSJ International Conference on Intelligent Robots and Systems (IROS)*, pages 5307–5314. IEEE, 2015.

[14] Q. Nguyen and K. Sreenath. Optimal robust control for constrained nonlinear hybrid systems with application to bipedal locomotion. In *2016 American Control Conference*, pages 4807–4813, July 2016.

[15] Ill W. Park, Jung Y. Kim, Jungho Lee, and Jun H. Oh. Online free walking trajectory generation for biped humanoid robot KHR-3(HUBO). *Proceedings - IEEE International Conference on Robotics and Automation*, 2006(May):1231–1236, 2006.

[16] Michael Posa, Cecilia Cantu, and Russ Tedrake. A direct method for trajectory optimization of rigid bodies through contact. *The International Journal of Robotics Research*, 33(1):69–81, 2014.

[17] M. J. Powell, A. Hereid, and A. D. Ames. Speed regulation in 3D robotic walking through motion transitions between human-inspired partial hybrid zero dynamics. In *IEEE International Conference on Robotics and Automation,*, pages 4803–4810. IEEE, 2013.

[18] I Michael Ross and Fariba Fahroo. A unified computational framework for real-time optimal control. In *Proceedings 42nd IEEE Conference on Decision and Control*, volume 3, pages 2210–2215. IEEE, 2003.

[19] K. Sreenath, H. Park, I. Poulakakis, and J. W. Grizzle. A compliant hybrid zero dynamics controller for stable, efficient and fast bipedal walking on MABEL. *The International Journal of Robotics Research*, 30(9):1170–1193, 2011.

[20] A. Wächter and L. T. Biegler. On the implementation of an interior-point filter line-search algorithm for large-scale nonlinear programming. *Mathematical programming*, 106(1):25–57, 2006.

[21] E. R. Westervelt, J. W. Grizzle, C. Chevallereau, J. H. Choi, and B. Morris. *Feedback control of dynamic bipedal robot locomotion*. CRC press Boca Raton, 2007.

[22] Hui-Hua Zhao, Wen-Loong Ma, Michael B Zeagler, and Aaron D Ames. Human-inspired multi-contact locomotion with AMBER2. In *ICCPS'14: ACM/IEEE 5th International Conference on Cyber-Physical Systems (with CPS Week 2014)*, pages 199–210. IEEE Computer Society, 2014.